Enhancement of breakdown voltage in AlGaN/GaN HEMT using air bridge recessed source filed plate

Padmavathi M[1], Manikandan M[2]

[1] *Research scholar, School of Engineering/ECE, Presidency University, Bangalore &*

Assistant Professor, Department of ECE, Dayanandasagar College of Engineering, Bangalore.

[2] *Assistant Professor, school of ECE, Presidency University, Bangalore*

padhushankar5@gmail.com,

manikandan.m@presidencyuniversity.in / email2mani86@gmail.com

Abstract.

The study introduces a technique to boost high-frequency AlGaN/GaN HEMTs breakdown voltages by applying an air-bridge recessed plate attached to the gate. This proposed technique solves the voltage breakdown performance problems that frequently occur in conventional GaN-based devices under high-frequency conditions. An air-bridge recessed source field (AB-FP) plate integration into the drain-gate junction changes the electric field distribution to decrease peak electric fields and boost breakdown voltages. The device performance characterization utilizes simulations together with experimental results that show how breakdown voltage improves significantly alongside maintained high-frequency operation.

Keywords. AlGaN/GaN HEMT; different Field Plate (FP); TCAD simulation; breakdown voltage.

1. INTRODUCTION

Research on HEMTs functions as the central subject of power electronic device advancement due to its ability to improve breakdown voltage and power conversion efficiency. The use of AlGaN/GaN, along with other III-V semiconductors featuring large band gaps, enables improved breakdown voltages while leading to higher efficiency rates. The combination of AlGaN/GaN HEMTs on SiC substrates results in devices that exhibit enviable values of Transconductance and switching speed alongside excellent breakdown characteristics suitable for high-power applications. The exceptional DC operational characteristics of AlGaN/GaN HEMTs make them excellent for power electronic applications since high-voltage and high-current applications benefit from their reliable performance. [1]. High channel mobility coupled with low parasitic capacitances Cgs and Cgd result in superior efficiency because they reduce switching losses, thus making AlGaN/GaN HEMTs outperform alternative material systems. These devices maintain high dependability for power applications because their surface and interface trapping effects remain reduced. High voltage performance suffers from current collapse issues that hinder the performance of GaN-based HEMTs [2].

The devices have achieved recent high breakdown voltages of over 1000 V using AlGaN/GaN HEMTs, but their production capabilities on GaN substrates remain limited due to both high manufacturing costs and production difficulties of GaN wafers. The absence of approved implantation techniques for GaN wafer technology exacerbates these problems even more [3]. Research must focus on alternatives like silicon (Si) and silicon carbide (SiC) as cheaper substrate materials since they deliver high breakdown voltage capabilities alongside satisfactory performance levels. The proposed AlGaN/GaN HEMT structure adopts SiC as its substrate to resolve the existing challenges. The AlGaN/GaN channel reduces ON resistance effectively, whereas the SiC substrate enables higher breakdown voltages at reduced production expenses, thus offering an appealing technological solution for the future generation of power devices [4].

2. STRUCTURE AND SPECIFICATIONS OF HEMT DEVICES

Figure 2.1. Displays GaN HEMT structures wherein the basic HEMT structure maintains a field plate absence followed by gate field plate (G-FP) and an air bridge recessed source field plate. The stack composition starts with SiC substrate followed by a 3µm buffer layer and continues with a 30nm GaN channel and 1 nm AlN spacer, then a 25 nm AlGaN barrier before finishing with a 2 nm GaN cap layer and 300 nm Si_3N4.[5].

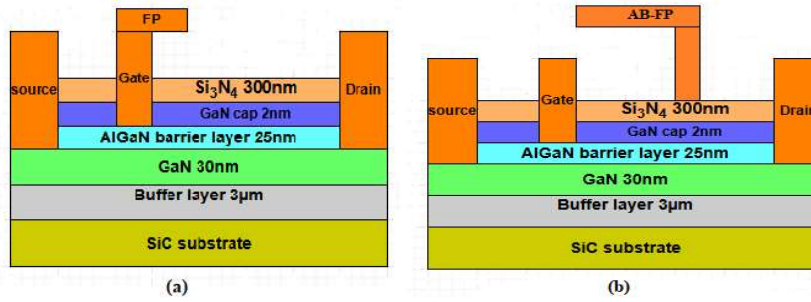

Fig.2.1. Schematic diagram of AlGaN/GaN HEMT with (a) with Gate Field Plate (b) with Air bridge recessed source Field Plate.

The simulation adopts the material properties for GaN and AlGaN according to the data found in Table 1. A calibration procedure was carried out for both the IMPACT SELB and POLARIZATION models to obtain appropriate breakdown operation and channel 2DEG concentration values. The interface trap generates its energy level that lies 0.8 eV below the conduction band edge [6]. The study utilizes contact traps which exist uniformly at every point throughout the materials with a density value of $2 \times 10^{12}/cm^2$. The buffer layer contains an acceptor trap concentration value of $1 \times 10^{18}/cm^2$ positioned 1eV below the conduction band energy level. The measurement of electron and hole capture cross section stands at $1 \times 10^{-15}/cm^2$ under degeneracy conditions where degeneracy equals one [7]. The simulation models SRH for carrier generation and recombination and combine FLDMOB with ALBRCT to explain mobility and saturation velocity behavior in addition to using GANSAT to model nitride-specific mobility characteristics [8]. SELB IMPACT carries out impact ionization simulations for avalanche breakdown, and the trap model configures trap effects alongside the FERMI model for establishing Fermi statistics and CALC.STRAIN model for calculating strain. The POLARIZATION model executes strain calculation tasks, which result from both spontaneous polarization effects and epipolar mismatch strains [9]. In HEMT devices, the electric field does not maintain a uniform distribution along the gate-drain region. The drain electrode edge section experiences a major electric field maximum when the external gate sinks to a potential different from the drain electrode [10]

Table 1: The simulation parameters were

Simulation parameter	GaN	AlGaN
Energy Bandgap	3.5eV	4.1eV
permittivity	9.6	9.5
Electron Mobility(μ_n)	1000cm^2/Vs	590cm^2/Vs
V_{sat} Saturation Velocity of electron	2.5x10^7(cm/s)	1.2x10^7(cm/s)
Density state of conduction band(Nc 300K)	2.3x10^{18}cm^3	2.1x10^{18}cm^3
Density state of valence band(Nv300K)	1.1x10^{19}cm^3	1.1x10^{19}cm^3

3. SIMULATION RESULTS.

3.1 DC characteristics

A physical simulator provides device validation because the simulated outputs match traditional field plate HEMT measurements. The air bridged field plate HEMT showcases 0.77 A/mm maximum drain current and 470 mS/mm maximum Transconductance as Figure 3.1(a) and (b) depicts. A device's input voltage and output current electrical properties correlate through Transconductance, which derives from drain-source current measurements. Fig.3.2. shows the air bridged plate structure developed in this study achieves breakdown voltages between 842.6 V and 1100.5 V. The G-FP measures 3µm, while the air-bridged recessed source FP extends to 18µm. The single G-FP and air bridged recessed source field plate produced breakdown voltages that exceeded basic structure with no field plate by factors of 3.2 and 3.8, respectively. The addition of G-FP produces breakdown voltages that surpass the no-FP structure by four times. Impact ionization acts as the fundamental mechanism that leads to the breakdown process [11]

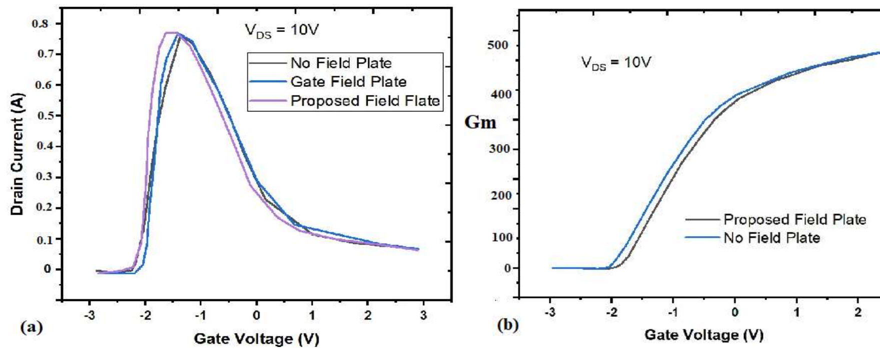

Fig.3.1. (a) the drain current and (b) transconductance

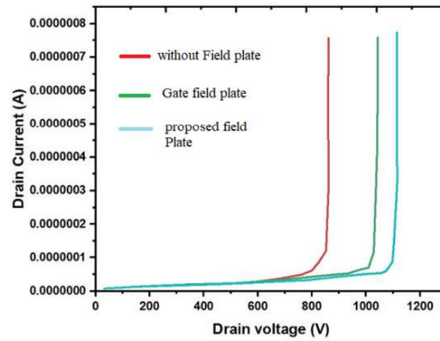

Fig 3.2. Breakdown voltage for different field plate

3.2. Transient characteristics

Multiple defects, such as surface lattice dislocations alongside dangling bonds and fabrication-related damage, result in numerous surface states that sit on top of AlGaN. Before passing via thermal emission, electrons leave the gate and tunnel over the metal/semiconductor contact because of heightened electric field stress that becomes active at the drain-side gate edge during OFF-state operation. Donor-like traps use electron injection to decrease 2DEG quantity, and the stretching electric field operates from drain to gate. The electric field control capability of AB-FP devices produces fewer trapped electrons when compared to basic and GFP structures in OFF-state operation conditions. The gate's edge electrical field weakness produces major electron reduction when gates turn on. The processes of electron emission, along with recombination, come to an end. The channel receives electrons as donor-like traps release their captured electrons, thus restoring them to the channel region. The ON-resistance rise ratio (Ron dynamic – Ron static)/Ron static serves as a research tool to assess the suppression capabilities of the no FP, GFP, and AB-FP structure devices while discussing the extent of collapse observed. Pulsed measurements demonstrate the results whereby a drain bias voltage V_{ds} increases from 20 V to 300 V by 20 V increments per test during OFF-state operations. The device switches between ON-state operation with $V_{gs} = 2$ V and OFF-state operation with $V_{gs} = -3$ V before returning to the $V_{gs} = 2$ V ON-state. The OFF state and both ON-states receive separation through a one-millisecond time boundary.

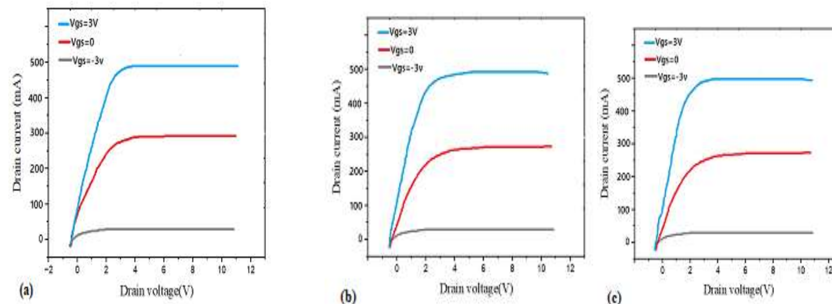

Fig.3.3 : voltage vs current characterstic of a) no FP b) gate FP c) Air bridged recessed source FP

Figure 3.3 demonstrates the output properties of three distinct field plate configurations. The gate voltage (V_g) fluctuates between -3 and 3V, and the source-drain voltage (V_{ds}) ranges from 0 to 12V. V_g= 3 V results in maximum saturation currents (I_{ds}) of no FP, G-FP, and AB-FP of 490 mA/mm, 511.1 mA/mm, and 528.7 mA/mm, respectively, according to the output curve. The little variation is associated with the two-dimensional electron gas density.

4. CONCLUSION

The research follows an organized process to enhance the device arrangements. Maximum breakdown voltages are obtained through different gate field plate lengths combined with source field plate lengths after analysing gate thickness and FP effective length. The research findings from character development matched the predictions produced through simulations for four devices that utilized various taped-off field plates. The device's DC characteristics experience minor changes from field plate construction, but its breakdown voltage and electric field intensity distribution pattern is affected by this structure. An Air-Bridge Field Plate integrated into the AlGaN/GaN HEMT device generates manufacturer-designed 2.52 mΩ.cm2 intrinsic ON-resistance with breakdown voltage reaching 1110 V. The device obtains elevated breakdown voltage performance by picking the correct length for field plates from suitable structural configurations

5. REFERENCES

[1]. Xing, H.; Keller, S.; Wu, Y.-F.; McCarthy, L.; Smorchkova, I.P.; Buttari, D.; Coffie, R.; Green, D.S.; Parish, G.; Heikman, S.; et al. Gallium nitride based transistors. J. Phys. Condens. Matter 2001, 13, 7139.

[2]. Eastman, L.; Mishra, U. The toughest transistor yet [GaN transistors]. IEEE Spectr. 2002, 39, 28–33.

[3]. Zhang, N.; Mehrotra, V.; Chandrasekaran, S.; Moran, B.; Shen, L.; Mishra, U.; Etzkorn, E.; Clarke, D. Large area GaN HEMT power devices for power electronic applications: Switching and temperature characteristics. In Proceedings of the IEEE 34th Annual Conference on Power Electronics Specialist 2003—PESC'03, Acapulco, Mexico, 15–19 June 2003; IEEE: Piscataway, NJ,USA, 2003; Volume 1.

[4]. Mishra, U.K.; Parikh, P.; Wu, Y.-F. AlGaN/GaN HEMTs-an overview of device operation and applications. Proc. IEEE 2002, 90,1022–1031.

[5]. Xing, H.; Dora, Y.; Chini, A.; Heikman, S.; Keller, S.; Mishra, U. High Breakdown Voltage AlGaN–GaN HEMTs Achieved by Multiple Field Plates. IEEE Electron Device Lett. 2004, 25, 161–163.

[6]. Kong, X.; Wei, K.; Liu, G.-G.; Liu, X.-Y. Improvement of breakdown characteristics of an AlGaN/GaN HEMT with a U-type gatefoot for millimeter-wave power application. Chin. Phys. B 2012, 21, 128501.

[7]. Moon, J.; Grabar, R.; Antcliffe, M.; Fung, H.; Tang, Y.; Tai, H. High-speed FP GaN HEMT with fT/fMAX of 95/200 GHz. Electron.Lett. 2018, 54, 657–659.

[8]. Zhang, Y.; Wei, K.; Huang, S.; Wang, X.; Zheng, Y.; Liu, G.; Chen, X.; Li, Y.; Liu, X. High-Temperature-Recessed Millimeter-Wave AlGaN/GaN HEMTs with 42.8% Power-Added-Efficiency at 35 GHz. IEEE Electron Device Lett. 2018, 39, 727–730.

[9]. Karmalkar, S.; Mishra, U. Enhancement of breakdown voltage in AlGaN/GaN high electron mobility transistors using a field plate. IEEE Trans. Electron Devices 2001, 48, 1515–1521.

[10] .He, J.; Cheng, W.C.; Wang, Q.; Cheng, K.; Yu, H.; Chai, Y. Recent Advances in GaN-Based Power HEMT Devices. Adv. Electron Mater. 2021, 7, 2001045. [CrossRef]

[11]. Kumar, V.; Kumar, S.; Maan, A.S.; Akhtar, J. Interfacial and structural analysis of MeV heavy ion irradiated SiC. Appl. Nanoscience 2021, 1–8. [CrossRef]